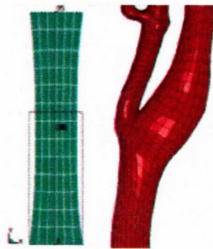


Task III Update: Carotid Artery Model

F. Scott Gayzik,
Joel D. Stitzel, Stefan M. Duma
January 23, 2006
Far Side Meeting
Melbourne, Australia

VIRGINIA TECH WAKE FOREST UNIVERSITY
School of Biomedical Engineering and Sciences



WAKE FOREST
UNIVERSITY
SCHOOL of MEDICINE
THE BOWMAN GRAY CAMPUS



VIRGINIA TECH - WAKE FOREST UNIVERSITY
CENTER FOR INJURY BIOMECHANICS

Overview

- Background and significance
- Modeling purpose and goals
- Mesh development
- Material model development
- Integration with THUMS model
- Publications current and planned
- Future work



Background and significance

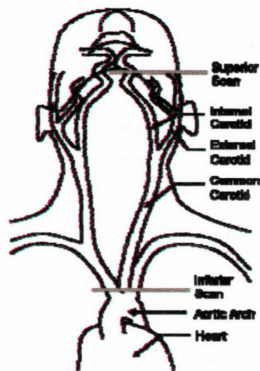
- Cervical artery dissection begins as a tear of the intimal lining
 - Over time → luminal occlusion → cerebral ischemia
- Internal carotid artery dissection (ICAD) is 3 to 5 times more frequent than vertebral artery dissection (Schievink et al. 1994, Haneline, et al. 2003)
- 30% of all ICAD cases are attributed to some form of trauma (Haneline and Lewkovich, 2005)

Modeling purpose and goals

- Analyze vehicle occupant safety in the case of side impact collisions
- Develop a robust material model and mesh
- Embed the carotid model in THUMS
- Incorporate into this model:
 - Strain rate dependence
 - Damage

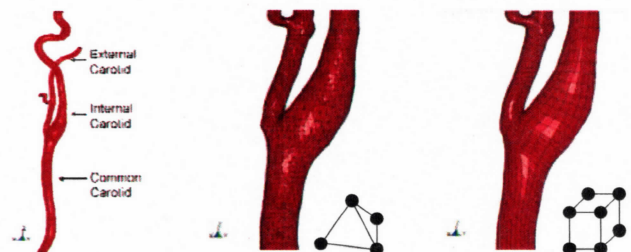
Mesh development

- Model constructed (CT) angiography of 57 year old male
- A total of 270 scans with slice thickness = 0.625mm
- Image data is from left carotid artery



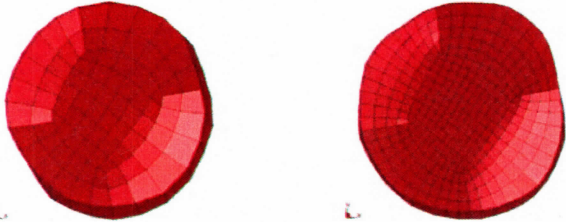
Mesh development

- Arterial lumen segmented, automatic mesh generated (volumetric)
- True Grid used to generate structured mesh around tetrahedral mesh



Mesh development

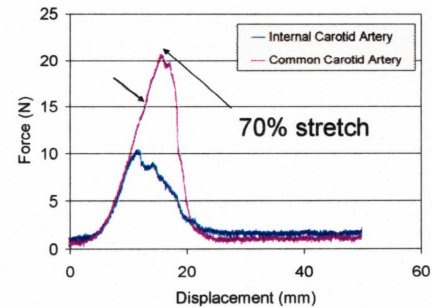
- Parametric meshing: painless mesh refinement
- Small change in volume and surface area
- Surface coated with shell elements



Common carotid cross sections, baseline mesh (left), double the elements (right)

Material model development

- Model strip test, compare outcome to uniaxial data
 - Human carotid data, Loading portion of curve used

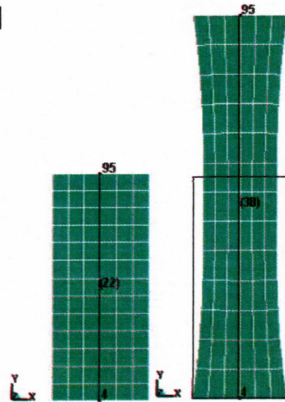


Specimen dimensions:

L = 22mm
W = 9.5mm
T = 1.77mm

Material model development

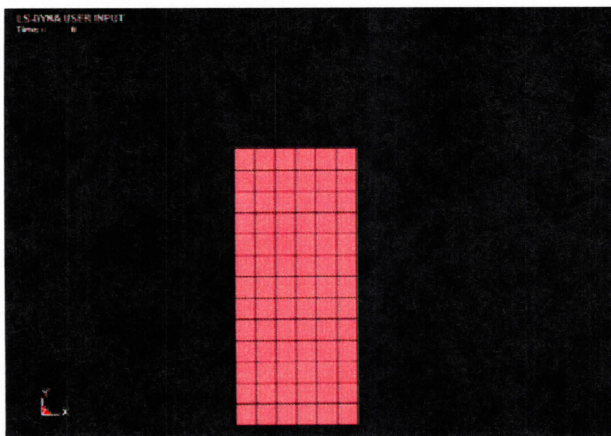
- Can the material model incorporate:
 - Large strain (70-80%)
 - Rate effects
 - Damage
- Is the model robust:
 - Parameter sensitivity?
 - Stability?



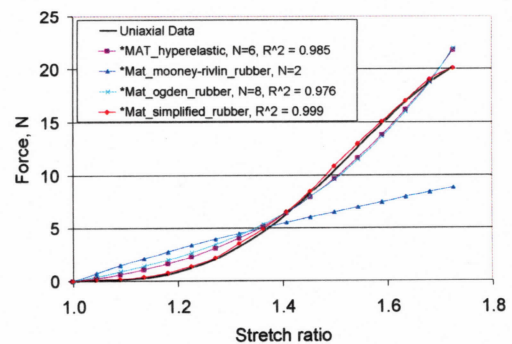
Material model development

- *MAT_mooney_rivlin
 - poor data fit, large strain instability
- *MAT_soft_tissue
 - stable, poor data fit, strong directional dependence
- *MAT_ogden_rubber
 - good data fit, large strain instability
- *MAT_hyperelastic_rubber
 - excellent fit, large strain instability
- *MAT_simplified_rubber
 - excellent fit, stable at large strain

Spot the instability



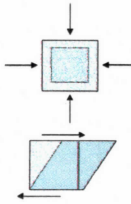
Data fit results, various models



MAT_simplified_rubber

- Uniaxial Data
 - Specimen dimensions
- Density, ρ [kg/m³]
- Bulk Modulus, K [MPa]
 - Resistance to change in volume
- Shear Modulus, G [MPa]
 - Resistance to shearing
 - Estimated via, $K, \nu=0.49$
- Limit stress for frequency independent, frictional damping, SIGF [MPa]
- Hourglass study

$$K = \frac{\Delta P}{\Delta V/V}$$

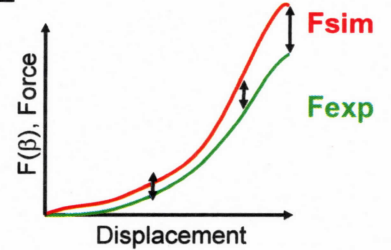
$$G = K \frac{3(1-2\nu)}{2(1+\nu)}$$


Evaluating goodness of fit

- Model response vs. experimental response used to evaluate goodness of fit.
- Goal of response optimization to minimize objective function E

$$E = \sum (F_{sim}(\beta_N) - F_{exp})^2$$

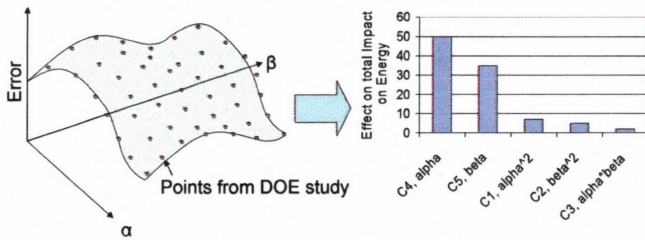
- E approaches zero, better fit



Design of experiment study used to determine high-impact parameters

- Let the material model have two parameters, α and β
- Design space outlines values of α and β
- A second order polynomial, P (Blue) is calculated by least squares fit to the data points from the design of experiment study (Dots)
- The coefficients are used in the Pareto plot

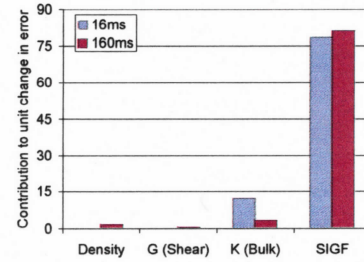
$$P = C_1\alpha^2 + C_2\beta^2 + C_3\alpha\beta + C_4\alpha + C_5\beta$$



Parameter study, *MAT_simplified_rubber

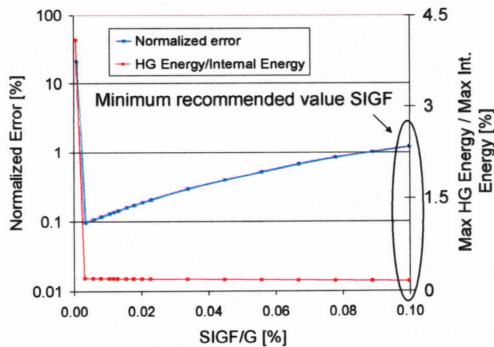
Full factorial parameter study :

- $\pm 25\%$ ρ, K, G and SIGF, from nominal values
- SIGF, K show largest effect model error between force v. ΔL



Isight software, Engineous software, Raleigh, NC

Effect of SIGF on goodness of fit

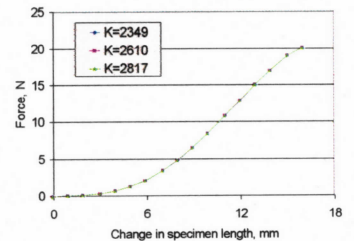


Error normalized by maximum force in specimen uniaxial test

Effect of bulk modulus

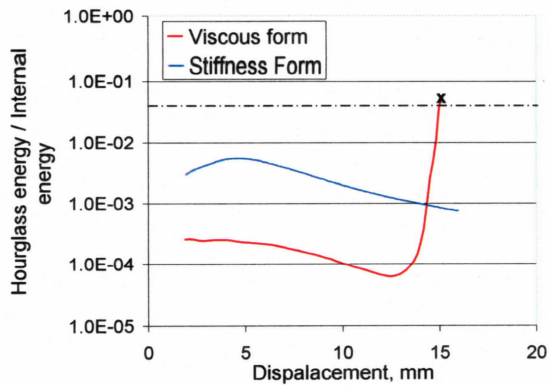
- Bulk modulus used¹, $K=2.61\text{GPa}$
- Bulk modulus of water, $K=2.0\text{GPa}$
- Effect of varying K $\pm 10\%$
- Shear modulus (G) estimated from bulk modulus

$$K = \frac{\Delta P}{\Delta V/V} \quad G = K \frac{3(1-2\nu)}{2(1+\nu)}$$



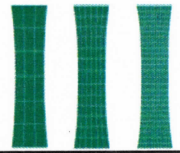
1. Bulk modulus of human aorta, from Duck, F.A., Physical properties of tissue, 1990

Hourglass control study



Mesh density study

- Mesh designed for roughly cubic elements shell side ~1.77mm
- Investigated for roughly 4-fold increase and decrease in elements
- Run time changed
- No change in accuracy of F v. D
 - Error 78 elements ~ 0.5
 - Error 312 elements ~ 0.5



Elements	18	78	312
Error	1.0	0.5	0.5
Run Time (min)	0.5	4	22

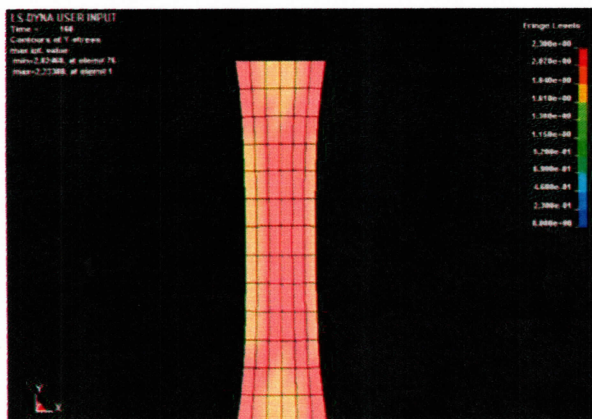
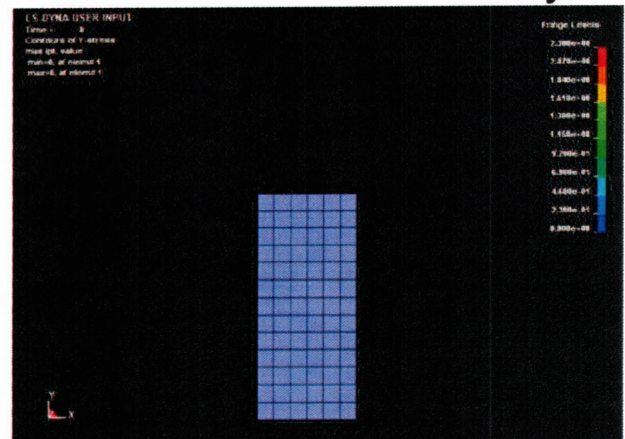
Run on Dell Optiplex GX620,
3.9GHz, 1GB RAM,
Termination time 160ms

Material model summary

- *MAT_simplified_rubber
 - Direct curve fit model
- Shell elements
- Model is robust
 - Parameter study
 - Mesh density study
- Strain rate effects and damage can be incorporated!
 - Enter curves at discrete strain rates
 - Damage function can be implemented

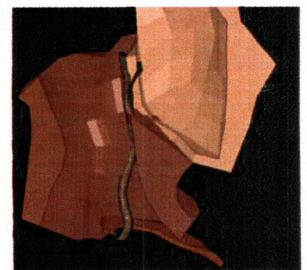
ρ	0.001	g/mm^3
K	2610	MPa, [N/mm ²]
G	5.2	MPa, [N/mm ²]
SIGF	0.04	MPa, [N/mm ²]
HG	Stiffness	

Material model summary



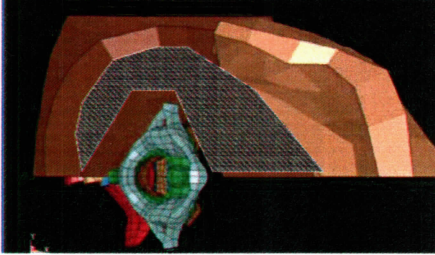
Integration with THUMS

- The carotid model will be embedded in THUMS
- Location validated by landmark data measures
 - C2, C4, C7
- Currently: re-meshing neck soft tissue



Integration with THUMS

- Mesh does not need to fill in space between the vertebrae
- Mesh will encompass the entire carotid, but leave space for vertebrae.



Current publication efforts and future work

- RMBS abstract accepted
- AAAM abstract submitted
- Incorporate rate effects and damage into *MAT_simplified_rubber
- Use THUMS model to investigate the effects of belt loading
- Submit entire study to a Biomechanics Journal
 - Clinical Biomechanics
 - J. App. Biomechanics

Thank you!

- Acknowledgments
 - Jim Day, LS-Dyna
 - Jeff Berger, LS-Dyna
 - MCW
- Questions?

VIRGINIA TECH WAKE FOREST UNIVERSITY
School of Biomedical Engineering and Sciences

WAKE FOREST
UNIVERSITY
SCHOOL of MEDICINE
THE BOWMAN GRAY CAMPUS

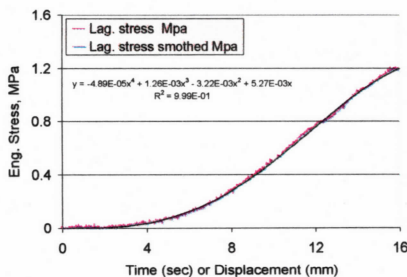
CIB
VIRGINIA TECH – WAKE FOREST UNIVERSITY
CENTER FOR INJURY BIOMECHANICS

Supplemental slides

- Data smoothing, preparation
- Physiologic stress state estimates
- Constitutive equations to selected models

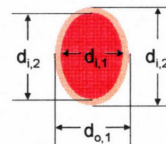
SSI: Data smoothing and preparation

- Data zeroed by subtracting average of first 50 points
- 4th order polynomial ($R^2=0.999$) fit to data
- Data points for Dyna taken from polynomial fit



SSII: Physiologic stress range

At both C5 and C6 the following 4 measurements are taken from CT scans of a 57 year old male:



$$\text{Average inner radius: } \bar{r}_{i,cx} = \frac{d_{i,1} + d_{i,2}}{2}$$

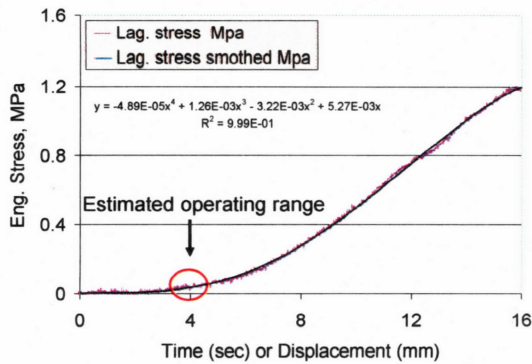
$$\text{Average outer radius: } \bar{r}_{o,cx} = \frac{d_{o,1} + d_{o,2}}{2}$$

$$\text{Average thickness: } \bar{t}_{cx} = \bar{r}_o - \bar{r}_i$$

$$\text{Longitudinal stress: } \sigma_L = \frac{P}{2} \left(\frac{\bar{r}_i}{\bar{t}} \right)$$

	C5	C6
$(\bar{r}_i/\bar{t})_{cx}$	6.2	5.1
$\sigma_{L,80\text{mmHg}}$ (kPa)	33.	27.
$\sigma_{L,120\text{mmHg}}$ (kPa)	49.	41.

Physiologic stress range on plot



SSIII: Constitutive equations to selected models

- Start with strain invariants

$$I_1 = \lambda_1^2 + \lambda_2^2 + \lambda_3^2$$

$$I_2 = \lambda_1^2 \lambda_2^2 + \lambda_2^2 \lambda_3^2 + \lambda_1^2 \lambda_3^2$$

$$I_3 = \lambda_1^2 \lambda_2^2 \lambda_3^2$$

$$J = \lambda_1 \lambda_2 \lambda_3 = \frac{V}{V_0}$$

- Stress = derivative of strain energy density function w.r.t. strain

$$\sigma_{ij} = \frac{\partial W}{\partial \epsilon_{ij}} = \frac{\partial W}{\partial I_k} \frac{\partial I_k}{\partial \epsilon_{ij}}$$

SSIII: Constitutive equations to selected models

- Hyperelastic Model

$$W(I_1, I_2, J) = \sum_{p,q=0}^n C_{pq} (I_1 - 3)^p (I_2 - 3)^q + W_H(J)$$

$$J_1 = I_1 J^{-1/3}$$

$$J_2 = I_2 J^{-2/3}$$

- Mooney-Rivlin Model

$$W(I_1, I_2, J) = A(I_1 - 3) + B(I_2 - 3) + C\left(\frac{1}{J^2} - 1\right) + D(I_3 - 1)^2$$

$$C = \frac{A+B}{2}$$

$$D = \frac{A(5\nu - 2) + B(11\nu - 5)}{2(1 - 2\nu)}$$

Mesh development for a finite element model of the carotid artery

F. Scott Gayzik^{1,2}, Josh C. Tan¹, Stefan M. Duma², Joel D. Stitzel^{1,2}

¹Wake Forest University School of Medicine, Medical Center Blvd, Winston-Salem, NC 27157

²Virginia Tech – Wake Forest University Center for Injury Biomechanics, Medical Center Blvd, Winston-Salem, NC 27157

Introduction

The internal branch of the left and right common carotid arteries and the vertebral arteries together are responsible for delivering blood to the brain. Disruptions in this blood supply lead to stroke, the third leading killer in the United States. The direct and indirect costs of stroke in the United States will reach \$56.8 billion in 2005 [1].

Of all strokes, 88% are ischemic [1] and of these, atherosclerosis is responsible for more than half. Sites of complex hemodynamics are associated with the formation of atherosclerotic plaques since the disease is commonly observed at arterial bifurcations and regions of high vessel curvature. Dissections of the carotid or vertebral artery account for 2% of ischemic strokes but larger percentages of stroke in young or middle aged patients (up to 10 to 25%) [2]. **Nearly 30% of all Internal Carotid Artery Dissections are attributed to some form of trauma, with blunt carotid artery injuries most commonly encountered in automobile crashes [3].**

Purpose

Understanding the complex biomechanics and fluid dynamics of the carotid artery is critical to developing interventions. Finite element analysis (FEA) and computational fluid dynamics (CFD) are widely used to investigate arterial mechanics. An important aspect of model development is the mesh of the geometry. The mesh refers to how a geometry is broken into discrete elements which are used in the finite element framework. By and large, the current research in this area is conducted using unstructured meshes comprised of tetrahedral elements.

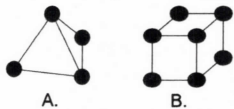


Figure 1. Element formulation examples. (A) 4-node tetrahedral element (B) 8-node hexahedral element

This research outlines a technique for developing a structured, hexahedral and parametrically-defined mesh of a the carotid artery. This mesh will be employed in future finite element analysis and computational fluid dynamic analysis studies to understand in greater detail the biomechanics of the artery.

Methods

The carotid artery model was constructed from a Computed Tomography (CT) angiography of 57 year old male patient. Images were taken using a Lightspeed Pro 16 Scanner (GE medical systems, Minneapolis, MN). A total of 270 slices were obtained, from the base of the jaw to the insertion of the artery to the aortic arch.

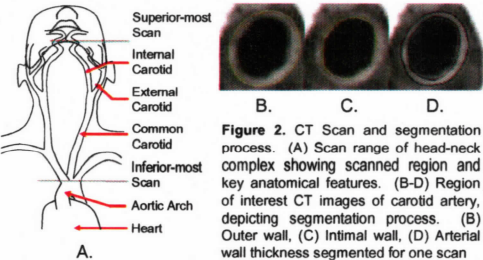


Figure 2. CT Scan and segmentation process. (A) Scan range of head-neck complex showing scanned region and key anatomical features. (B-D) Region of interest CT images of carotid artery, depicting segmentation process. (B) Outer wall, (C) Intimal wall, (D) Arterial wall thickness segmented for one scan

Methods, Cont.

The lumen of the vessel was segmented using Mimics (Materialise, Leuven, Belgium). An automatic surface meshing algorithm was used to form a tetrahedral mesh along the intimal surface of the artery. This mesh was exported to TrueGrid (XYZ Scientific Technologies, Inc., Livermore, CA) for hexahedral mesh generation. Splines were drawn circumferentially and longitudinally along the surface of the tetrahedral mesh using existing nodes. Surfaces were created using these splines as edges. Parametric meshing is accomplished by mapping each surface of the model to a simple geometric block. The hexahedral mesh is defined on the simplified block and projected back to the complex surfaces of the carotid model. The structured mesh was coated with shell elements. The protocol for use of geometry from clinical medical images was reviewed by Wake Forest's Internal Review Board and approved prior to commencement of work.

Results

The results are summarized in Figures 3-5. The total volume and surface area of the structured mesh are found in Table 1. The parametric meshing capability of this approach allows for the mesh of the complex structure to be adjusted with minimal additional effort. Figure 4 demonstrates this capability, showing a cross section of the common carotid artery with the baseline mesh and a revised mesh with twice the number of elements.

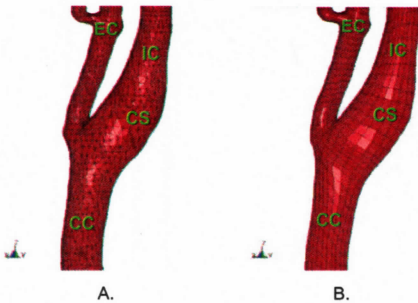


Figure 3. Detail in the area of the bifurcation, showing (A) tetrahedral mesh, and (B) hexahedral mesh. Common carotid (CC), internal (IC), external (EC) carotid arteries and the carotid sinus (CS).

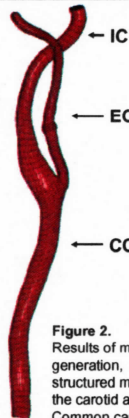


Figure 2. Results of mesh generation, structured mesh of the carotid artery. Common carotid (CC), internal (IC), external (EC) carotid arteries

Discussion

A structured mesh of the carotid artery is a valuable asset in conducting a fluid dynamic or solid mechanic analysis. Since the mesh is created parametrically, the task of refining mesh density is simplified. Changing the number of elements along a dimension of the model is accomplished by changing a parameter and recompiling the input file. It is accepted that models employing structured meshes generally provide more accurate solutions and are more computationally efficient than models employing tetrahedral elements. It is also possible to encounter material models that are not formulated for use with tetrahedral elements and two-dimensional triangular shells.

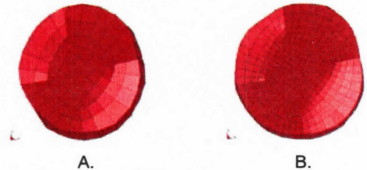


Figure 4. Cross section of carotid model showing mesh density. (A.) Mesh baseline, (B.) Mesh with double the number of elements

Table 1. Mesh volume and surface area measurements

	Volume, cm ³	Surface Area, cm ²
Hexagonal mesh	7.59	51.2
Tetrahedral mesh	7.71	51.9
% Difference	+1.56	-1.35

With any model reconstructed from medical images error is present, however we believe no significant increase in geometrical error is introduced by meshing the model with hexahedral elements. Similar studies have estimated the error due to image segmentation at $\pm 8\%$ in both area and volume. [4, 5]. This segmentation error estimate is much larger than the difference in volume and surface area moving from a tetrahedral to hexahedral mesh (Table 1). **A brief survey of the literature shows that structured meshes are yet to be fully integrated into the most recent research, with some studies directly citing the complex geometry of the carotid as the reason for using unstructured meshes [4, 6, 7].**

No computational models on the role blunt trauma to the head-neck complex plays in spontaneous carotid artery dissection were found, despite the estimated mortality and neurological morbidity of this injury of 40% and 40-80% respectively [3]. Future research will employ this carotid model in such investigations.

Acknowledgements

Thanks to Mike Burger for his expertise using True Grid to the carotid artery model. The funding for this research has been provided in part by an Australian Research Council linkage Grant.

References

- American Heart Association. *Heart Disease and Stroke Statistics – 2005 Update*. Dallas, TX: American Heart Association; 2005.
- W. I. Achieving, *N Engl J Med*, vol. 344, pp. 898-906, 2001.
- B. D. Stemper, N. Yoganandan, and F. A. Pintar, *J Biomech*, vol. 38, pp. 2491-6, 2005.
- H. F. Younis, et al., *Biomech Model Mechanobiol*, vol. 3, pp. 17-32, 2004.
- M. R. Kazempour-Mofrad, et al., *Ann Biomed Eng*, vol. 32, pp. 932-46, 2004.
- H. F. Younis, et al., *Ann Biomed Eng*, vol. 31, pp. 995-1006, 2003.
- Z.-Y. Li, et al., *Journal of Biomechanics*, vol. In Press, Corrected Proof.

